Secondary Structure of Ovalbumin Messenger RNA

Nguyen T. Van, James W. Holder, Savio L. C. Woo,
Anthony R. Means, and Bert W. O'Malley*

ABSTRACT: The secondary structure of highly purified ovalbumin mRNA was studied by automated thermal denaturation techniques and the data were subjected to computer processing. Comparative studies with 20 natural and synthetic model nucleic acids suggested that the secondary structure of ovalbumin mRNA possesses the following features: the extent of base pairing of ovalbumin mRNA is similar to that found in tRNAs or ribosomal RNAs; the secondary structure of ovalbumin mRNA is more thermolabile than any of the model compounds tested, including the copolymer poly(A-U); ovalbumin mRNA does not have extensive G-C rich stems as found in tRNAs or ribosomal RNAs; the base composition of the double-stranded regions reveals 54% G-C residues which was significantly higher than that noted in the whole molecule (~41.5% G-C). The presence of 46% A-U pairs in short stems of about five base pairs would have a very large destabilizing effect on the secondary structure of ovalbumin mRNA. However, at 0.175 M monovalent cations and 36 °C most of the secondary structure of ovalbumin mRNA is preserved. These data suggest that the double-stranded regions in ovalbumin mRNA are of sufficient length to provide the necessary stability for maintaining the open loop regions in an appropriate conformation which may be required for the biological function of ovalbumin mRNA. Furthermore, the lability of the double-stranded regions in ovalbumin mRNA may also be important for the biological function of this mRNA.

Several classes of RNAs, such as viral RNAs, ribosomal RNAs, 5S RNAs, and tRNA, possess highly ordered secondary structures which might be required for their biological functions (Fresco et al., 1963; Levitt, 1969; Min Jou et al., 1972; Simsek and Rajbhandary, 1972; Weissmann et al., 1973; Murray, 1974). Until recently, little information was known concerning the secondary structure of eucaryotic messenger RNAs. This was primarily due to the difficulty encountered in purifying the large amounts of specific mRNA necessary for these physical studies.

Recently our laboratory has reported purification on a preparative scale and partial characterization of ovalbumin mRNA (Woo et al., 1975; Rosen et al., 1975). This has allowed us to undertake detailed physical studies of the secondary structure of ovalbumin mRNA in the hope of correlating its structure with its biological function. We have found that thermal denaturation techniques which make extensive use of the first derivative of hypochromicity with respect to temperature were highly informative. These methods not only allowed us to demonstrate the existence of base-paired regions in ovalbumin mRNA, but also to rule out the presence of highly G-C rich stems in ovalbumin mRNA similar to what has been observed with tRNAs and ribosomal RNAs. In addition, the analysis of hypochromicity at several wavelengths coupled with rapid renaturation methods have yielded information concerning both the sequence organization and base distribution in ovalbumin mRNA.

Materials and Methods

Nucleic Acids. The RNAs of biologic origin utilized in this study are listed in Table I along with information related to their origin, base composition, and molecular weight. Criteria for determining the purity of ovalbumin mRNA have been reported previously (Woo et al., 1975; Rosen et al., 1975). To summarize briefly, the mRNA migrated as a single band in two different gel electrophoretic systems under denaturing conditions and fingerprinting of ^{125}I-labeled ovalbumin mRNA demonstrated the absence of ribosomal RNA contaminants. Finally, following translation in a cell-free wheat germ translation system, all detectable newly synthesized protein co-electrophoresed with authentic ovalbumin.

Purified rabbit globin mRNA was the generous gift of Dr. J. B. Lingrel. It consisted of an equal mixture of the purified α- and β-globin mRNA chains (Morrison et al., 1974).

Rabbit reticulocyte tRNA, 18S rRNA, and 28S rRNA were purified by zonal centrifugation in a sucrose gradient as described previously (Holder, 1973). The $tRNA_{fMet}$ was a gift of the Oak Ridge National Laboratories. MS2 viral RNA and synthetic nucleic acid polymers were purchased from Miles Laboratory. Poly[r(G-C)] was purchased from Boehringer, Mannheim, Germany.

In most experiments, the nucleic acids were precipitated from ethanol and centrifuged, and the pellet was redissolved in 0.01 M Tris[1], pH 7, containing 0.0001 M EDTA at a final concentration of 20 A_{260}/ml. Buffers used in this study were freshly prepared and filtered through Millipore filters (AAWP 0.3 μm) or alternatively, centrifuged at 5000 rpm for 15 min to remove residual particulate matter.

Thermal Denaturation. Solutions used in thermal denaturation studies were also degassed for 5 min by a constant flow of helium (chromatographic grade). This procedure minimized the formation of bubbles since helium has a positive coefficient of solubilization with temperature (Felsenfeld and Sandeen, 1962). Overlaying the solution with silicon oil (Dow 200) and covering the cuvette with an air-tight Teflon stopper were found to be essential for the prevention of bubble formation.

Thermal denaturation of the nucleic acids was performed

† From the Department of Cell Biology and Center for Population Research, Baylor College of Medicine, Houston, Texas 77025. *Received July 22, 1975.* This work was supported by NIH Grants HD-8188 and HD-7857, American Cancer Society Grant BC-101, and a grant from the Robert A. Welch Foundation (Q-611).

[1] Abbreviations used: EDTA, ethylenediaminetetraacetic acid; Tris, tris(hydroxymethyl)aminomethane; uv, ultraviolet; Hb, hemoglobin; IDS, index of double strandedness; RNA*, RNA obtained from hen oviduct; RNA**, RNA obtained from rabbit reticulocyte; Ov, oviduct.

TABLE I: Base Composition and Molecular Weight of Six Naturally Occurring RNAs.

Nucleic Acids	(G + C) %	Mol Wt	No. of Nucleotides In the Poly(A) Tail
Ov mRNA*	41.5[a]	650 000[a]	62[a]
Hb mRNA**	52.3[b]	170 000[b]	65[d]
MS2 RNA	52[c]	1 110 000[g]	
tRNA**	60.4[d]	25 000[g]	
18S rRNA**	56.5[e]	700 000[f]	
28S rRNA**	67.7[e]	1 580 000[f]	

[a] Woo et al., 1975. [b] Williamson, 1971. [c] Strauss and Sinsheimer, 1963. [d] Holder, 1973. [e] Gould et al., 1966. [f] Loening, 1968. [g] Calculated from the number of nucleotides: 3300 nucleotides for MS2 and 70–80 nucleotides for tRNAs.

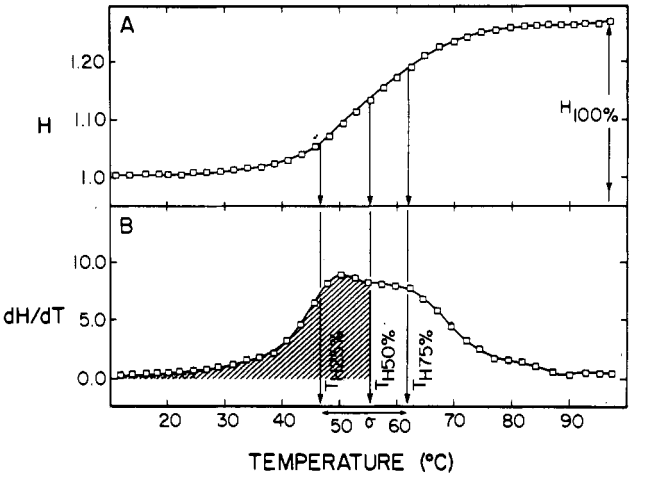

FIGURE 1: Thermal denaturation data (H and dH/dT) of *E. coli* tRNA. The ionic strength of the buffer is 0.1 M KCl, 0.001 M Tris at pH 7, 0.0001 M EDTA. Each curve consists of about 250 data points. Only one in every five points is represented by a symbol for simplicity of presentation. (A) Plot of $H = A(T)/A(10\ °C)$ as a function of temperature. $A(T)$ and $A(10\ °C)$ are the absorbances measured at T and 10 °C, respectively; $H_{100\%} = H(100\ °C) - 1$ is hypochromicity of tRNA in 0.1 M KCl. (B) First derivative of H with respect to temperature dH/dT. $T_{H50\%}$ is the melting temperature T_m at which 50% of the RNA is denatured. σ is the half breadth of the melting transition which is the temperature range between $H_{25\%}$ and $H_{75\%}$.

at both 260 and 278 nm in an automatic, temperature-programmed and digitally recording spectrophotometer (the optical component of which is a Gilford prism monochromator) constructed to give a level of performance identical with that described by Ansevin and Brown (1971). Temperature was monitored by a YSI thermistor probe No. 44201 immersed in the reference solution. This probe was calibrated with a series of four thermometers calibrated by the National Bureau of Standards. To ensure good heat transfer, the cuvette holder was machined from a large piece of brass and the variation in the four slots of the cuvette holder was determined to be less than 0.1 °C. Heating was performed at a rate of 0.8 °C/min, from 10 ± 1 to 100 ± 1 °C. Starting the denaturation at a temperature much lower than room temperature was found essential to maintain maximum base pairing in RNAs, especially at low ionic strength (Goldstein et al., 1972). The hypochromism of RNAs measured under these conditions is significantly higher than the hypochromism measured in the normal range (25–100 °C). On the other hand, if denaturation is not carried out to 100 °C, stems in RNAs containing a high G-C content are uncompletely denatured, resulting in an apparent low hypochromism. Reproducibility in wavelength setting was also found to be important in order to obtain consistent hypochromic data. This is especially true at 278 nm where the absorption spectrum of RNAs has a particularly steep slope. The wavelength scale of the Gilford spectrophotometer was calibrated with the sharp peak of the holmium oxide filter at 2795 Å.

Data points were taken every one-third of 1 °C and an average experimental curve consisted of about 200 to 250 points. Only one in five symbols was plotted for simplicity of presentation but the line connecting the symbols passed through all the experimental points. Data plotting and computation of the hypochromicity and the derivative of hypochromicity with respect to temperature were done by a computer (IBM 360). All data were corrected for the thermal expansion of solutions.

Uv Spectra Determinations and the Protocol for Cooling Experiments. The uv spectra of nucleic acid samples were obtained with a double-beam Cary 118 spectrophotometer. Quick-cooling experiments were performed in a jacketted cuvette (1-cm light path) connected to two circulating water baths. The temperatures of these baths were set at 10 and 90 °C, respectively. A system of clamps was used so that switching from one bath to another could be completed within 30 s. Since the heat capacity of the cuvette was very small, it was found that the temperature of the sample could be cooled to room temperature within 1 min. When complete denaturation spectra were measured, the high-temperature bath was set at 110 °C and used to heat a Cary jacketted cuvette holder. The temperature in the melting cuvette (monitored by a probe) reached a plateau at 99 ± 1 °C within 5 min. Two recordings were made for each spectrum and the published denatured spectra were replicates of two independent determinations.

Definitions and Symbols. Native RNA possesses secondary structure and is hypochromic with respect to its basic components, the four bases. Therefore, when a solution of RNA is heated, an increase in absorption, i.e., hyperchromism, is observed. When hyperchromicity is defined as the ratio $H(T) = A_T/A_{T_0}$ where A_T is the absorbance at temperature T and A_{T_0} is the absorbance at the starting temperature T_0 (which is 10 ± 1 °C), $H(T)$ measures the percent denatured RNA at temperature T. When T = 100 °C, the denaturation is assumed to be complete and $H(100\ °C) - 1$ is equal to the percent hypochromism of native RNA with respect to its single-stranded state. The latter is defined as a state where base stacking and pairing are absent. This hypochromism obtained by thermal denaturation is generally lower than the total hypochromism measured with respect to the mononucleotide state of the RNA (Mahler et al., 1964).

As an illustration, Figure 1 shows a typical plot of H (panel A) and the derivative dH/dT, of H with respect to temperature (panel B) of *Escherichia coli* tRNA in 0.1 M KCl. Also shown are: (1) the hypochromicity of *E. coli* tRNA with respect to its single-stranded state, which is equal to $H_{100\%}$ measured at the end of the denaturation and is generally carried out at 100 ± 1 °C; (2) the T_m which is the temperature corresponding to $H_{50\%}$; and (3) σ, the half-width of the melting range, which is the temperature range between $H_{25\%}$ and $H_{75\%}$.

Results

Base Pairing in Ovalbumin mRNA. To evaluate the extent of base pairing in ovalbumin mRNA, the total hypochromicity at 260 nm was compared with the hypochromicity of double-stranded and single-stranded model compounds (Table II). At 260 nm, the total hypochromicity of ovalbumin mRNA was

TABLE II: Hypochromicity at 260 and 278 nm and Index of Double Strandedness (IDS) of 14 Nucleic Acids.[a]

Class	Nucleic Acids	H_{260nm} (100%)	H_{278nm} (100%)	Ratio H_{278}/H_{260}	IDS
A	Ov mRNA	28	29	1.04	26
	Hb mRNA	29	38	1.31	16
	MS2	28	37	1.32	25
	$tRNA_{fMet}$	30	49	1.63	49
	18S rRNA**	31	40	1.29	18
	28S rRNA**	27	42	1.56	11
B	Poly[r(A-U)]	68	9	0.13	700
	Poly(dG-dC)	20	70	3.5	800
	Various DNAs	30-55	35-62	0.7-1.8	150-400
C	Poly(rU)	<1	<1	*c*	<0.1
	Poly(rG)[b]	<1	<1	*c*	<0.1
	Poly(rC)	14	28	2	0.8
	Poly(rA)	28	0	0	1.0
D	Random sequences				
	Poly[r(A,U,G,C)]	18	27	1.5	3

[a] To facilitate comparison, the model compounds are grouped in 4 classes: (A) mixture of the double-stranded and single-stranded structures; (B) perfect duplexes; (C) single-stranded structure; (D) random sequence poly[r(A,U,G,C)]. To obtain comparable hypochromicity values, it is imperative to begin the melt at a low temperature to ensure maximum base pairing and to terminate the melt at 100 °C to complete the denaturation of high G-C stems. [b] Does not denature between the range 10-100 °C. [c] Cannot be calculated accurately.

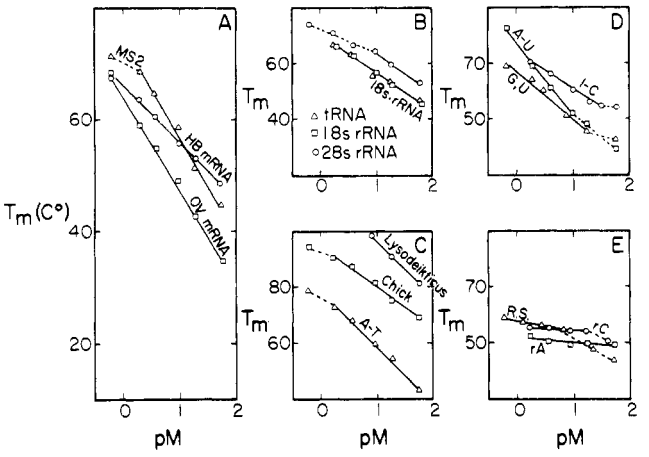

FIGURE 2: Variation of melting temperature T_m with ionic strength. (A) (□) Ov mRNA* (17 °C/pM); (○) Hb mRNA** (11 °C/pM); (△) MS2 (16 °C/pM). (B) (□) 18S rRNA** (13 °C/pM); (○) 28S rRNA** (10 °C/pM); (△) tRNA** (13 °C/pM). (C) (□) Chick DNA (15 °C/pM); (○) *Micrococcus lysodeikticus* (20 °C/pM); (△) poly[d(A-T)] (20 °C/pM). (D) (□) Poly[r(A-U)] (26 °C/pM); (○) poly[r(I-C)] (15 °C/pM); (△) poly[r(G-U)] (13 °C/pM). (E) (□) Poly(rA) (1.5 °C/pM); (○) poly(rC) (2 °C/pM); (△) poly[r(A,U,G,C)] (5 °C/pM). The slope in Celsius degree per pM is indicated in parentheses. Only data joined by a solid line were included in the computation of the least-squares regression line. The slopes of poly(rU) and poly(rG) are small <1 °C and are not included.

similar (within 2%) to the hypochromicity of all natural RNAs tested at ionic concentrations of 0.1-0.25 M KCl. The increase in absorbance with temperature was measured over the standard range of 10-100 °C. Under the same conditions, the hypochromicities of poly(A-U) and poly(G-C) were respectively 68 and 20%, whereas the hypochromicity of poly(I-C) and other double-stranded nucleic acids was 30-55%. However, as expected, the hypochromicity of the single-stranded polyribonucleotides was quite small with the exception of poly(A) which is known to possess a structure containing a large amount of base stacking.

Base pairing can also be demonstrated by the dependency of T_m on the ionic concentration of the melting medium. These data are presented in Figure 2. The linearity of T_m with pM (the logarithm of the reciprocal ionic concentration) was excellent for the two eucaryotic mRNAs over a wide range of concentration (0.01-1.5 M). The slope of T_m vs. pM for each nucleic acid is indicated in the legend of Figure 2. The slope of perfect duplexes was greater than 15 °C/pM, whereas the slope for single-stranded RNAs was small and generally not significant. As can be seen in Figure 2, the slopes for ovalbumin mRNA and MS2 RNA were as great as those observed for the double helical nucleic acids, but the slope for Hb mRNA was closer to the slopes of tRNAs and rRNAs.

We were also able to determine the amount of base pairing in ovalbumin mRNA which was present under different temperatures and ionic conditions. This value was estimated from the area under the derivative profile of dH/dT plotted vs. temperature. For example, *E. coli* tRNA was half-denatured at 55 °C when the ionic strength was 0.1 M KCl as noted by the shaded area under the derivative profile shown in Figure 1, panel B. On the other hand, at the same ionic strength and 25 °C, only 3% of the secondary structure was lost. Figure 3 shows the derivative profiles of the two eucaryotic mRNAs and a viral RNA obtained at three different ionic strengths. At all three concentrations, the ovalbumin mRNA appears to be more thermolabile than the other two RNAs. At low ionic concentrations, ovalbumin mRNA was half-denatured at room temperature (panel A) but at 0.175 M KCl and 36 °C, more than 90% of the secondary structure was preserved.

The width of the melting transition was calculated from the curves and employed to estimate the extent of base pairing in ovalbumin mRNA. This parameter is inversely proportional to the cooperativity observed during the melting of nucleic acids. In all cases, a high cooperativity is associated with double-stranded structures. Information related to the width of the melting transition, σ, is shown in Figure 4. All double-stranded helical nucleic acids showed a very high cooperativity (panel D) during melting, i.e., a small σ (σ = 1-5 °C), whereas

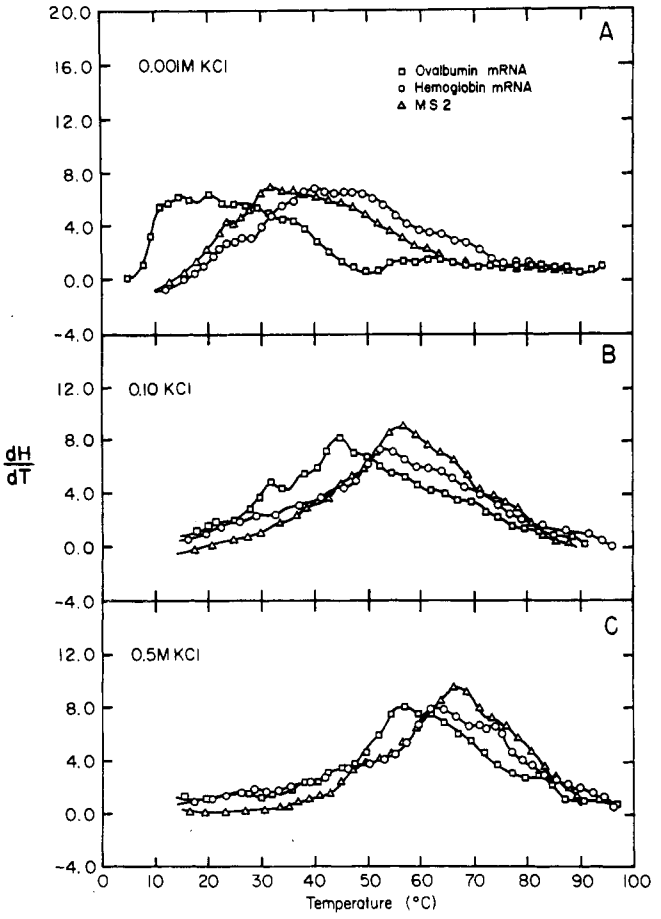

FIGURE 3: Derivative profiles at 260 nm of H vs. temperature for 2 eucaryotic mRNA and 1 viral RNA at indicated ionic strength. (A) At 0.001 M KCl. Half of ovalbumin mRNA is denatured at room temperature at this low ionic concentration (represented by the area under its derivative profile to the left of 25 °C). (B) At 0.1 M KCl. (C) At 0.5 M KCl. At physiological concentration (0.175 M), the derivative profile should lie between the derivative profiles in panels B and C, respectively. It can be estimated that at this concentration, less than 10% of the ovalbumin mRNA is denatured at 36 °C.

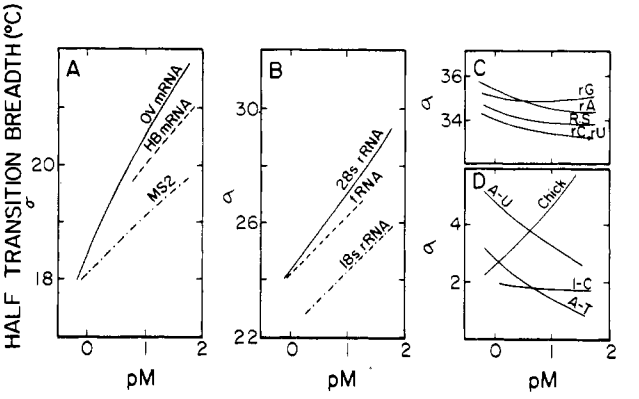

FIGURE 4: Variation of the half breadth of the melting transition, σ with ionic strength. A: Ov mRNA (—); Hb mRNA (- - -); and MS2 RNA (- · - · -). B: 28S rRNA* (—); tRNA* (- - -); and 18S rRNA* (- · - · -). C: Poly(rA), (rC), (rU), (rG), and poly[r(A,U,G,C)] were identified with plot directly below. D: Poly[r(A-U)], poly[r(I-C)], chick liver DNA, and poly[d(A-T)]. Standard deviations of σ data shown in panels A, B, C, D are ±0.5, ±1, ±1.5, and ±0.3 °C, respectively.

the melting transition was broadest (panel C) for the single-stranded RNAs (σ = 34–35 °C). The random sequence poly(A,U,G,C) which can have very short base pairing in 40–60% of the molecule (Fresco et al., 1960; Gralla and DeLisi, 1974) also exhibited broad melting transition (Figure 4, panel C). The eucaryotic mRNAs and the viral RNA showed an intermediate cooperativity (σ = 18–22 °C) which was greater than the melting cooperativity observed for ribosomal RNAs (σ = 22–29 °C). The negative slope of σ with pM was also observed with naturally occurring DNAs but not with synthetic single-stranded or double-stranded polymers.

Since double strandedness correlates directly with hypochromicity, sensitivity of T_m with pM and melting cooperativity, it is informative to combine these three parameters in a single indicator, the index of double strandedness (IDS) defined as follows:

$$\text{IDS} = \frac{H_{260\text{nm}}\ (\%) \times \text{slope}\ T_m/\text{pM}\ (°\text{C})}{\sigma\ (°\text{C})}$$

The index of double strandedness for 14 nucleic acids is shown in the last column of Table II. It is evident that all single-stranded model compounds exhibit an IDS of 1 or less and all double-stranded model compounds show an IDS larger than 100. The IDS of ovalbumin mRNA is 26.4 which is in the middle of the range for all naturally occurring RNAs (i.e., 11–49) and is significantly higher than the IDS of the random polymer poly(A,U,G,C). This result suggests that the double-stranded regions in ovalbumin mRNA might be longer than what is assumed for a random polymer (i.e., 1–3 base pairs).

Practical Considerations for Choosing Model Compounds for the Duplex Regions of Ovalbumin mRNA. From published models of naturally occurring RNAs (Levitt, 1969; Min Jou et al., 1972; Simsek and Rajbhandary, 1972; Weissmann et al., 1973; Murray, 1974), these RNAs are represented as duplex populations separated by single-stranded regions. The average length of the duplexes is 4–5 base pairs. Short oligonucleotides are commercially available but the thermal stability of these compounds is far below what has been observed with the short duplexes in naturally occurring RNAs (Doty et al., 1959; Fink and Crothers, 1972; Gralla and Crothers, 1973a,b), thus making them unsuitable as model compounds for the later. The copolymers poly[r(A-U)] and poly[r(G-C)] are suitable model compounds if one can assume as in earlier works (Felsenfeld and Sandeen, 1962; Fresco et al., 1963; Cox, 1966) that each base pair contributes independently to the denaturation spectrum and that nearest neighbor effect is negligible. The copolymer poly[r(A-U)] is a better model compound than the equimolecular mixture of poly(rA) and poly(rC) used earlier by Fresco et al. (1963) since the denaturation of this mixture shows a significant contribution from the unstacking of the poly(rA) strand. The copolymer poly[r(G-C)] obtained from Boehringer (Mannheim, Germany) is very thermostable and does not denature in the range 10–100 °C, thus rendering itself unsuitable in some experiments. However, we found that the compound poly(dGdC) which exhibits an almost identical denaturation spectrum as does poly[r(G-C)] in the range 255–290 nm (Figure 9, panel C) and which is more thermolabile than poly[r(G-C)] can be a suitable model compound within this wavelength range. To test the assumption that the single-stranded structures do not contribute significantly to the denaturation spectrum (Gould and Simpkins, 1969), we also used the $tRNA_{fMet}$ as a model compound for the G-C duplexes in ovalbumin mRNA. From sequence and x-ray crystallography data, this G-C rich RNA appears as a mixture of 3 hairpin loops and 1 short duplex of 4–7 base pairs each. Only 2 A-U pairs are present in a total of 21 base pairs (Simsek and Rajbhandary, 1972). $tRNA_{fMet}$ can

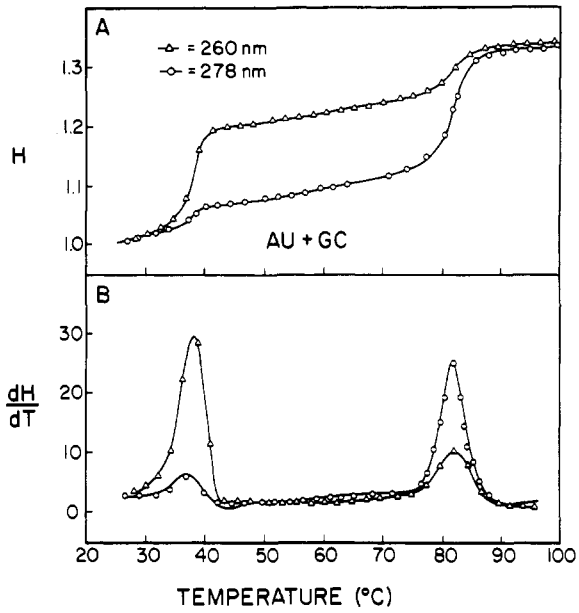

FIGURE 5: Thermal denaturation data of a mixture of poly[r(A-U)] and poly(dGdC). The ratio of A-U/G-C in this mixture is 0.9. The buffer is 0.02 M KCl, 0.001 M Tris, pH 7, 0.0001 M EDTA. (A) Hypochromicity curve: 260 nm (open triangle); 278 nm (open circle). (B) Derivative dH/dT: 260 nm (open triangle); 278 nm (open circle).

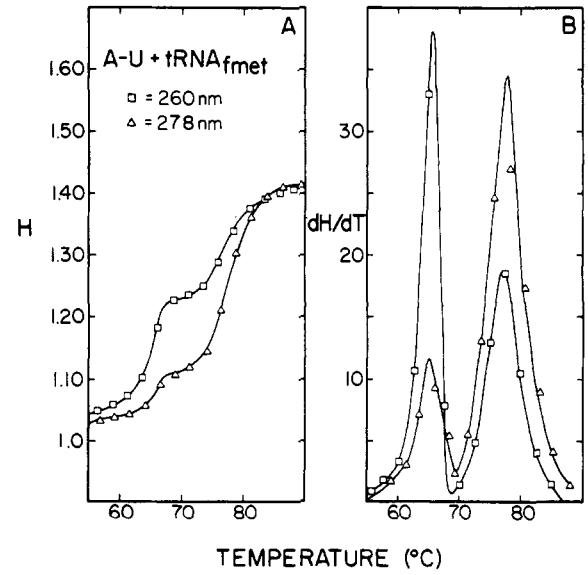

FIGURE 6: Thermal denaturation data of a mixture of poly[r(A-U)] and $tRNA_{fMet}$. The mixture contains 45 μM of A-U and 76 μM of $tRNA_{fMet}$ (nucleotide to nucleotide) in 0.1 M KCl, 0.001 M Tris pH 7, 0.0001 M EDTA. (A) Hypochromicity curve: 260 nm (open square); 278 nm (open triangle). (B) Derivative dH/dT: 260 nm (open square); 278 nm (open triangle).

therefore serve as a model for the short G-C rich duplexes in naturally occurring RNAs.

Base Composition and the Distribution of A-U and G-C Pairs in Double-Stranded Regions. To determine if there were populations of duplex structure with widely different base composition in eucaryotic mRNAs, the thermal denaturation profile was measured at two wavelengths (260 and 278 nm). The 278-nm wavelength was chosen as a more sensitive indication of the denaturation of G-C pairs than of A-U pairs (Cox, 1966). The hypochromicity at 278 nm for the natural RNAs is shown in Table II, column 3. A good correlation existed between $H_{\%}$ at 278 nm vs. G-C content of RNAs as expected. All natural RNAs showed an increase in $H_{100\%}$ at 278 nm when compared with the $H_{100\%}$ at 260 nm. The percent increase ranged from 5% for the ovalbumin mRNA to 30% for Hb mRNA, MS2 RNA, and 18S rRNA and was as high as 60% for 28S rRNA and $tRNA_{FMet}$.

To assure an accurate interpretation of the derivative profiles of the eucaryotic mRNAs, the following two experiments were performed. First, a mixture of poly(A-U) and poly(dGdC) at a well defined ratio (A-U:G-C, 0.9:1.0) was denatured to yield equal total $H_{100\%}$ at both wavelengths, 260 and 278 nm. The rationale behind choosing this ratio is to reproduce the equality of H_{260nm} and H_{278nm} observed in ovalbumin mRNA. The hypochromicity of A-U and G-C at 278 nm is listed in Table II. For A-U, the hypochromicity at 260 nm was seven times greater than the $H_{100\%}$ at 278 nm. In contrast, when G-C was examined, an inverse relationship existed with $H_{100\%}$ at 278 nm being 3.5 times larger than $H_{100\%}$ at 260 nm. This effect was best illustrated by the hypochromicity curves and the derivative profiles shown in Figure 5 which depict the thermal data for a mixture of 0.9 part A-U to 1 part G-C. It is evident that this ratio ensured equal total hypochromicity at 260 and 278 nm. The denaturation curves were biphasic and the derivative profiles were bimodal at both wavelengths. They also showed identical T_m. The relative height of the peaks 278 nm/260 nm was also reversed at the two wavelengths. This experiment demonstrated that a mixture of A-U and G-C melted biphasically and that the melting of the A-U and G-C pairs were best observed at 260 and 278 nm, respectively. Furthermore, a high G-C peak is also characterized by the high ratio of H_{278nm}/H_{260nm} peaks.

The purpose of the next experiment was to demonstrate that the existence of the imperfections does not invalidate the conclusions drawn from the previous experiment, i.e., the existence of G-C rich stems can still be revealed by the derivative profiles at 278 nm notwithstanding the presence of base mismatching or loops. Figure 6 contains the thermal data for a mixture of poly(A-U) and $tRNA_{fMet}$ at a ratio of 45 μM of A-U to 76 μM of $tRNA_{fMet}$ (nucleotide to nucleotide). This ratio was found sufficient to ensure equal H_{260nm} and H_{278nm}. It is evident that, except for a reduction in the T_m and a broadening of the G-C peaks, results similar to those shown in Figure 5 were obtained when the long poly(dGdC) polymer was replaced by a mixture of hairpin loops with short G-C stems. Thus in the light of the two experiments described above, we propose that the derivative profiles of H vs. temperature at 260 and 278 nm can be used to detect G-C rich stems in naturally occurring RNAs. The results of experiments of this nature are shown in Figure 7. It is well known that 28S rRNA possesses G-C stems which contain a high G-C content (Gould and Simpkins, 1969). We therefore examined the derivative profiles of 28S rRNA at 260 and 278 nm (Figure 7F). As can be seen, the profiles were plurimodal, and the areas of the two G-C rich peaks with maximums at 72 and 85 °C were 30 and 35%, respectively, of the total area. The derivative profile determined using rabbit reticulocyte tRNA (Figure 7D) revealed that the G-C rich (i.e., thermostable) peak area represented about 65% of the total area. However, the derivative profiles of the Hb mRNA, MS2 RNA, and 18S rRNA did not show distinct thermal populations but rather an overlapping of several populations (Figure 7B,C,E). The area under the large G-C rich peak (represented by a maximum at 80–85 °C) was about 10% for these three RNAs. Except for a small peak with a maximum near 80 °C, the derivative profiles for ovalbumin mRNA were very similar at both wavelengths. Furthermore, the derivative profile of ovalbumin mRNA was

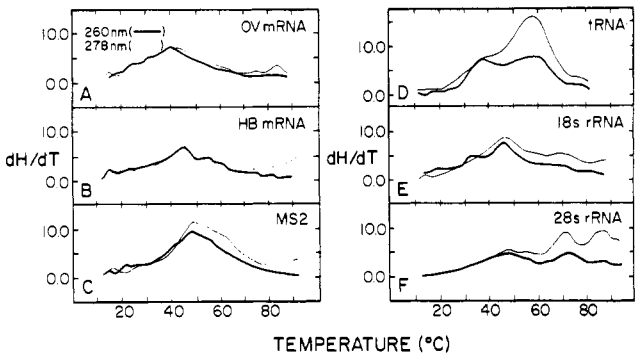

FIGURE 7: Derivative profiles dH/dT at 260 and 278 nm for six naturally occurring RNAs. Buffer: 0.08 M KCl, 0.001 M Tris, pH 7, 0.0001 M EDTA. Thick line: 260 nm. Thin line: 278 nm.

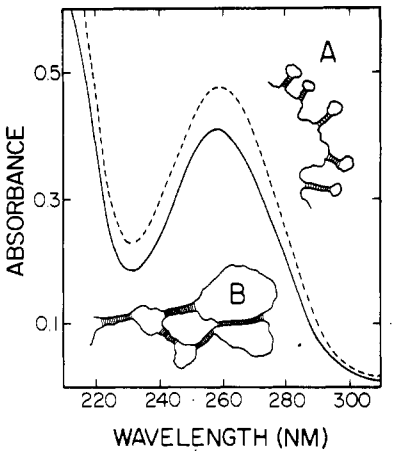

FIGURE 8: Room temperature and 90 °C spectra of ovalbumin mRNA. Buffer: 0.2 M KCl, 0.001 M Tris, 0.0001 M EDTA. Solid line: room temperature. Interrupted line: 90 °C. Repeated (up to six times) heating and cooling in the range 20–90 °C yielded coincidental spectra. Model A showed base pairing between neighboring sequences and model B involved refolding and pairing between distant sequences.

unimodal, suggesting the absence of distinct populations of double-stranded sequences containing widely different base compositions.

Sequence Organization in Ovalbumin mRNA. The experiments shown in the previous sections were designed to examine the extent of base pairing and the G-C composition in different duplex populations (i.e., the existence of high G-C stems) but did not provide information on the nature of the double-stranded regions. Double-stranded regions can be formed by hairpin loops which involve interactions between neighboring sequences (model A, Figure 8) or conversely base pairing between distant sequences which result from refolding (model B). Another possibility is that of intermolecular base pairing. Both the rate and the degree of renaturation can be used to investigate the nature of the base pairing within ovalbumin mRNA. Figure 8 shows the uv spectra of ovalbumin mRNA as determined at both room temperature and at 90 °C. The sample was quick cooled (within 1 min) and the spectrum of the cooled sample was recorded. This process was repeated six times and the spectra of the cooled or reheated sample were always coincidental with the initial recordings. When the change in absorbance was monitored at one wavelength, a simultaneous recording of the absorbance and the temperature showed that the change of absorbance followed the change in temperature within 2 s. In order to demonstrate that all renaturations were intramolecular rather than intermolecular reactions, short path length cuvettes (2 mm) were used in order to achieve concentrations of samples up to ten times those normally used. Identical rapid-cooling spectra at these higher concentrations were also obtained, suggesting that model A (Figure 8) is more likely than model B. Thus our data suggest that the base pairing present in ovalbumin mRNA results primarily from intramolecular interactions.

Base Composition in the Duplex Regions of Ovalbumin mRNA. The base composition of the duplex regions in ovalbumin mRNA can be calculated from the denaturation spectrum as described by Fresco et al. (1963). This technique has been utilized by several workers (Felsenfeld and Sandeen, 1962; Fresco et al., 1963; Cox, 1966) to estimate the base composition of both DNAs and RNAs. It assumed that each base pair contributes independently to the denaturation spectrum and that nearest neighbor effect is negligible. Figure 9A shows the denaturation spectra of poly[r(A-U)] and poly[r(G-C)] and the spectra of various mixtures of A-U and G-C calculated from the experimental spectra of pure A-U and pure [r(G-C)] (the denaturation spectrum of [r(G-C)] was taken from Fresco et al., 1963). The validity of such calculations, which is based on eq 1 of Fresco et al. (1963), has been demonstrated in several laboratories (Fresco et al., 1963; Cox, 1966) and was confirmed in our laboratory with several mixtures of poly[r(A-U)] and poly(dGdC). The denaturation spectra shown in Figure 9A reveal an isosbestic point at 244 nm where the denaturation spectrum is independent of A-U/G-C ratio. If the ratio ($\Delta E_{262nm}/\Delta E_{244nm}$) of the peak heights at 262 and 244 nm is plotted against the G-C percent of the mixture, a straight line is obtained (Figure 9B). If the same ratio is obtained for an unknown RNA, the base composition of the latter can be calculated from the line shown on Figure 9B. The denaturation spectrum of ovalbumin mRNA is illustrated in Figure 9D. Also shown is a spectrum (solid line) calculated for a mixture of A-U/G-C (0.94:1). It is evident that the agreement between the actual and the calculated denaturation spectra is remarkable. When an actual mixture of poly(A-U) and poly(dGdC) in the ratio of A-U/G-C = 1 is denatured, the denaturation spectrum of this mixture is very similar to the denaturation spectrum of ovalbumin mRNA in the range 255 to 295 nm (Figure 9D). The difference observed below 255 nm is due to the difference in the denaturation spectra of poly[r(G-C)] and poly(dGdC) below 255 nm. This result indicates that poly(dGdC) can be used as a model for the G-C pairs in RNAs at least in the range 260–300 nm. The ratio of $\Delta E_{262nm}/\Delta E_{244nm}$ for ovalbumin mRNA is 1.22 corresponding to 53% G-C. The denatured spectrum of the poly-[r(A,U,G,C)] is much lower than the corresponding spectrum for ovalbumin mRNA and the ratio $\Delta E_{262nm}/\Delta E_{244nm}$ is equal to 1.1, indicating that G-C pairs are predominant in the "random" sequence. This result is also consistent with the high H_{278nm}/H_{260nm} observed with the random sequence (Table II).

Discussion

Evidence for Base Pairing Regions within Ovalbumin mRNA. We have demonstrated the existence of double helical region in ovalbumin mRNA by three different parameters: hypochromicity, sensitivity of T_m with pM, and melting cooperativity.

Although these three parameters correlate well with double strandedness, they are also dependent on other factors. First, hypochromicity can be large in the unstacking of poly(rA) and poly(rC); second, the sensitivity of T_m vs. pM is dependent on base composition and is larger with A-U pairs; last, the melting

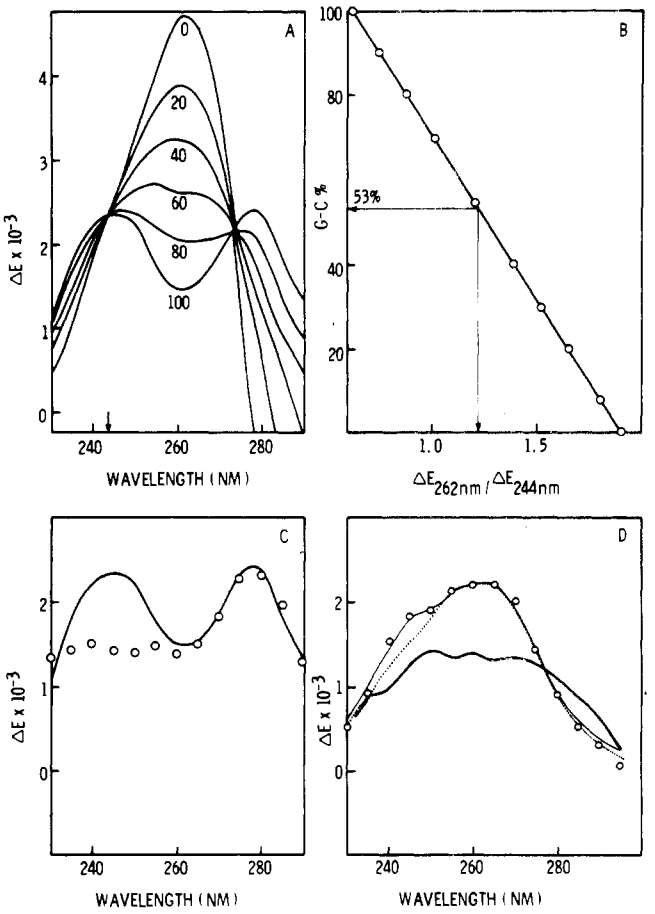

FIGURE 9: Base composition of the duplexes in ovalbumin mRNA. (A) Denaturation spectra of 100% A-U (0) and 100% G-C (100). The curves in between represent mixture of A-U and G-C and the number next to each curve represents the percent G-C in the mixture. The G-C curve was taken from Fresco et al. (1963). The A-U curve was measured differentially with a solution of poly[r(A-U)] in 0.1 M KCl, 0.001 M Tris, pH 7, 0.0001 M EDTA at 98 °C measured against the same solution maintained at 10 °C as reference in a double-beam Cary 118 spectrophotometer. The other curves were calculated from the A-U and G-C curves. (B) Plot of G-C percent as a function of the ratio of ΔE_{262nm} to ΔE_{244nm}; 244 nm is the isosbestic wavelength in panel A. A ratio of 1.22 corresponds to 53% G-C. (C) Denaturation spectrum of poly(dGdC) plotted on the same scale as the denaturation spectrum of poly[r(G-C)] taken from Fresco et al. (1963). Open circle: poly(dGdC) in 0.02 M KCl, 0.001 M Tris, 0.0001 M EDTA. Poly[r(G-C)]: solid line. (D) Denaturation spectra of ovalbumin mRNA and an equimolecular mixture of poly[r(A-U)] and poly(dG-dC). Open circle: Ov mRNA in 0.1 M KCl, 0.001 M Tris, 0.0001 M EDTA. Solid line: Calculated denaturation spectrum for a mixture of 34% A-U and 36% G-C. Dotted line: Denaturation spectrum of a mixture containing 20 μM A-U and 20 μM dGdC, respectively. Thick solid line: Denaturation spectrum of poly[r(A,U,G,C)]. The $\Delta E_{262nm}/\Delta E_{244nm}$ ratios for Ov mRNA and random copolymer are 1.22 and 1.1, respectively. The techniques described above do not give an accurate estimate of base composition for tRNAs where hydrogen bonds responsible for tertiary folding are substantial.

cooperativity is larger with copolymers or mixture of complementary homopolymers than with naturally occurring DNAs, notwithstanding that their perfect duplex nature is the same. However, these factors cannot negate our earlier conclusion that ovalbumin mRNA contains secondary structures as duplexes for the following reasons: (1) the unstacking effect of the poly(A) tail which represents only 4% of the bases in ovalbumin mRNA is likely to be small; (2) the difference in the slope of T_m vs. pM between A-U and G-C pairs is only a factor of two whereas the slope for ovalbumin mRNA is one order of magnitude higher than the slope for single-stranded model compounds; (3) the lower melting cooperativity for DNAs is still six times higher than the melting cooperativity for single-stranded model compounds and is due to a known cause: the difference in base composition of different sequences in naturally occurring DNAs. The index of double strandedness (IDS) which combines these three parameters in a single indicator differs by one order of magnitude between single-stranded model compounds and RNAs and by two orders of magnitude between single-stranded structures and duplexes, respectively, thus making these three classes of nucleic acids clearly distinct.

The random sequence copolymer poly(A,U,G,C) shows an IDS of 3 which is intermediate between the IDS of single-stranded polyribonucleotides (IDS $\leq$ 1) and all the other naturally occurring RNAs (IDS = 11-49). As such poly(A,U,G,C) clearly constitutes a separate class. One likely explanation is that the duplexes in the random sequence are shorter than what are generally found in naturally occurring RNAs which include ovalbumin mRNA (e.g., 1-3 base pairs vs. 4-5 base pairs).

Sequence Organization in Ovalbumin mRNA. The derivative profiles of $d\dot{H}/dT$ for ovalbumin mRNA show clearly that extensive highly G-C rich regions are absent. If the latter were present, they would be revealed as peaks demonstrable at high temperature which exhibit grossly different heights in the derivative profiles at 260 and 278 nm, respectively. This is clearly the case for tRNAs and 28S rRNA. In the 28S rRNA, the presence of G-C rich populations extends the melting range to higher temperature resulting in a decrease in melting cooperativity and IDS. It is therefore necessary to use the IDS only as a qualitative indicator since there is no reason to believe that there is more secondary structure in ovalbumin mRNA than in 28S rRNA. By comparing the derivative profiles at 260 and 278 nm, it was estimated that less than 4% of the sequences in ovalbumin mRNA are G-C rich (represented by the area of the small peak with maximum near 80 °C).

When the same analysis was applied to Hb mRNA, MS2 RNA, and 18S rRNA, the data revealed that about 10% of their base pairs existed as stems which were rich in G-C as compared with 35% for 28S rRNA. By the same token, tRNA has about 65% of its bases organized in G-C rich stems but with a lower overall G-C content than the stems containing the highest G-C stems in 28S rRNA (as shown by a lower T_m, 60 vs. 83 °C). It is interesting to note that, in ovalbumin mRNA, Hb mRNA, and MS 2 RNA, distinct populations with abrupt changes in G-C composition do not exist as has been observed with 28S rRNA.

The renaturation kinetics of ovalbumin mRNA support models in which base paired regions are formed between neighboring sequences (model A, Figure 8) rather than by extensive refolding and base pairing between distant sequences (model B, Figure 8). Intermolecular base pairing is ruled out as a result of both the rapid renaturation and the lack of dependency of the renaturation rate on the concentration of ovalbumin mRNA. Although the rate of chain growth can be extremely rapid, in the 10^{-6} s/mol range (Porschke, 1974), the renaturation rate of ovalbumin mRNA is certainly limited by the rate of nucleation which must be slow as a result of the high number and the shortness of the duplexes. Since the absorbance monitoring technique is only accurate to 1%, our results cannot rule out a limited amount of base pairing between some distant sequences. Specifically, pairing between the poly(A) tail at the 3′ end and a potential oligo(U) sequence at the 5′ end of the molecule to form a circular configuration

has recently been suggested by Brawerman (1975) and may not have been detected by our methods.

Base Composition of the Duplex Regions in Ovalbumin mRNA. Three remarkably consistent values for the percent G-C of the duplex regions in ovalbumin mRNA were obtained with three different approaches. First, theoretical calculation after Fresco et al. (1963) (using the denatured spectra in Figure 9A) produced a denaturation spectrum identical with the denaturation spectrum obtained for ovalbumin mRNA when the ratio of A-U/G-C is 0.94 (i.e., 51.5% G-C). Second, a 1:1 mixture of poly(A-U) and poly(dGdC) also yielded an identical denaturation spectrum in the range 260–290 nm where poly(dGdC) and poly[r(G-C)] showed similar spectral properties. Third, the G-C content of ovalbumin mRNA calculated from the extinction ratio (Figure 9B) was also 53%. These results coupled with the fact that a mixture of 0.9 A-U to 1 G-C (Figure 5) yielded similar $H_{278nm}/H_{260nm} = 1$ indicated that the percent G-C in the duplex regions of ovalbumin mRNA is 50–54%. The correctness of this estimate depends on the accuracy of the denaturation spectra shown in Figure 9A. The denaturation spectrum for A-U pairs was obtained with an alternating copolymer poly[r(A-U)]. The base pairing of such a copolymer must be close to 100%; therefore, the denaturation spectrum for A-U shown in Figure 9A is accurate on a molar basis. On the other hand, the denaturation spectrum of the copolymer poly[r(G-C)] used by Fresco et al. (1963) might not be known on a molar basis since base mismatching is possible. However, the denaturation spectrum of poly(dGdC) (perfect duplex) is very similar to the denaturation spectrum reported by Fresco et al. (1963) for poly[r(G-C)] in the range 260–320 nm. These observations suggest that the base pairing in the sample described by Fresco et al. (1963) might be close to 100%.

Secondary Structure in Ovalbumin mRNA at Physiological Conditions. The derivative profiles of ovalbumin mRNA as a function of ionic strength reveal that at least 90% of the secondary structure is preserved at 0.175 M ionic strength and 36 °C. The difference in the IDS and in the denaturation spectrum of the random polymer poly[r(A,U,G,C)] with respect to ovalbumin mRNA suggests that the double-stranded regions in the random sequence should be shorter than what was found in ovalbumin mRNA. It has been suggested by Fresco et al. (1960) that 40–60% of the bases in a random sequence can be paired, although with average length of only 1–3 base pairs. It is therefore evident that the duplex regions in ovalbumin mRNA must be longer than the average length of a random sequence double helix to explain the large difference in denaturation spectra, sensitivity of T_m vs. pM, and melting cooperativity. If this assumption is correct, this would bring the average length of the double helices in ovalbumin mRNA to at least 4–5 base pairs. This also is the average length found in tRNAs and is sufficient to maintain the appropriate conformation in the open loop region for specific pairing such as in codon–anticodon interactions.

The thermolability of ovalbumin mRNA may have an important consequence for its biological function. While the stems can provide the necessary rigidity required to maintain the open loops in an accurate conformation, they can also be denatured with minimum energy. Although the molecular size of ovalbumin mRNA is 50% larger than required to code for ovalbumin (Woo et al., 1975), it is unlikely that all the base-paired regions in ovalbumin mRNA are structural. Presumably they are also in the region of the mRNA which is translated into ovalbumin. A structure which would permit lability in the double-stranded regions of eucaryotic mRNA may be important for both the initiation of protein synthesis and peptide elongation.

In conclusion the following general statements concerning the secondary structure of ovalbumin mRNA have emerged from our thermal denaturation studies: (1) ovalbumin mRNA possesses an amount of secondary structure which is similar to that found in tRNAs and ribosomal RNAs; (2) its secondary structure is quite thermolabile but, at physiological conditions, more than 90% of its secondary structure is preserved; (3) ovalbumin mRNA does not have extensive G-C rich stems as found in tRNAs or ribosomal RNAs; (4) the presumed length of the double-stranded regions is about 4–5 base pairs, which is sufficient to maintain the correct conformation in the open loops; (5) the double helical regions are most likely formed by hairpin loops between neighboring sequences and the composition of the base paired regions is approximately 50–54% G-C. Since the overall base composition of ovalbumin mRNA is known to be low in G-C, it can be predicted that the open loop regions should be extremely rich in A-U.

Recently, the secondary structure of globin mRNA was investigated by alkaline hydrolysis, nuclear digestion, and thermal denaturation (Holder and Lingrel, 1975). This eucaryotic mRNA was found to have 55–62% of its nucleotides in base pair form. The G-C content of the duplexes was found to be similar to the G-C content of 18S rRNA.

Acknowledgments

We acknowledge Dr. A. T. Ansevin of the Department of Physics, M.D. Anderson Hospital and Tumor Institute, for the use of the computer program, Dr. Jeffrey M. Rosen for several useful comments and reading the proof, and Mr. Tim Yu for excellent technical assistance.

References

Ansevin, A. T., and Brown, B. W. (1971), *Biochemistry 10,* 1133–1142.

Brawerman, G. (1975), personal communication.

Cox, R. A. (1966), *Biochem. J. 98,* 841–857.

Doty, P., Boedtker, H., Fresco, J. R., Haselkorn, R., and Litt, M. (1959), *Proc. Natl. Acad. Sci. U.S.A. 45,* 482–499.

Felsenfeld, G., and Hirschman, S. Z. (1965), *J. Mol. Biol. 13,* 407–427.

Felsenfeld, G., and Sandeen, G. (1962), *J. Mol. Biol. 5,* 587–610.

Fink, T. R., and Crothers, D. M. (1972), *J. Mol. Biol. 66,* 1–12.

Fresco, J. R., Alberts, B. M., and Doty, P. (1960), *Nature (London) 188,* 98–101.

Fresco, J. R., Klotz, L. C., and Richards, E. G. (1963), *Cold Spring Harbor Symp. Quant. Biol. 28,* 83–90.

Goldstein, R. N., Stefanovic, S., and Kallenbach, N. R. (1972), *J. Mol. Biol. 69,* 217–236.

Gould, H. J., Arnstein, H. R. V., and Cox, R. A. (1966), *J. Mol. Biol. 15,* 600–618.

Gould, H. J., and Simpkin, H. (1969), *Biopolymers 7,* 223–239.

Gralla, J., and Crothers, D. M. (1973a), *J. Mol. Biol. 73,* 497–511.

Gralla, J., and Crothers, D. M. (1973b), *J. Mol. Biol. 78,* 301–319.

Gralla, J., and DeLisi, C. (1974), *Nature (London) 248,* 330–332.

Holder, J. W. (1973), Ph.D. Thesis, The University of Cincinnati.

Holder, J. W., and Lingrel, J. B. (1975), *Biochemistry 14,*

4209-4215.
Levitt, M. (1969), *Nature (London) 224,* 759-763.
Loening, U. E. (1968), *J. Mol. Biol. 38,* 355-365.
Mahler, H. R., Kline, B., and Mehrotra, B. D. (1964), *J. Mol. Biol. 9,* 801-811.
Min Jou, W., Haegeman, G., Yalbaert, M., and Fiers, W. (1972), *Nature (London) 237,* 82-88.
Morrison, M. R., Brinkley, S. A., Gorski, J., and Lingrel, J. B. (1974), *J. Biol. Chem. 249,* 5290-5295.
Murray, K. (1974), Biochemistry of Nucleic Acids, Burton, K., Ed., Baltimore, Md., University Park Press.
Porschke, D. (1974), *Biophys. Chem. 2,* 83-96.
Rosen, J. M., Woo, S. L. C., Holder, J. W., Means, A. R., and O'Malley, B. W. (1975), *Biochemistry 14,* 69-78.
Simsek, M., and Rajbhandary, U. L. (1972), *Biochem. Biophys. Res. Commun. 49,* 508-515.
Strauss, J. H., Jr., and Sinsheimer, R. L. (1963), *J. Mol. Biol. 7,* 43-54.
Weissmann, C., Billeter, M. A., Goodman, H. M., Hindley, J., and Weber, H. (1973), *Annu. Rev. Biochem. 42,* 303-328.
Williamson, R., Morrison, M., Lanyon, G., Eason, R., and Paul, J. (1971), *Biochemistry 10,* 3014-3021.
Woo, S. L. C., Rosen, J. M., Liarakos, C. D., Robberson, D. L., Choi, Y. C., Busch, H., Means, A. R., and O'Malley, B. W. (1975), *J. Biol. Chem. 250,* 7027-7039.

Interaction Specificity of the Anthracyclines with Deoxyribonucleic Acid†

E. J. Gabbay,*,‡ D. Grier,§ R. E. Fingerle,§ R. Reimer,§ R. Levy,# S. W. Pearce,¶ and W. D. Wilson‡‡

ABSTRACT: The interaction specificity of salmon sperm DNA with various derivatives of daunorubicin has been studied. The results of binding, viscometric, ^1H nuclear magnetic resonance (NMR), flow dichroism, DNA template inhibition, rates of dissociation, and circular dichroism studies are found to be consistent with an intercalation mode of binding of the anthracycline ring as has been shown by other investigators. Moreover, it is observed that (i) strength of binding, (ii) the ease of dissociation of DNA–anthracycline complexes, and (iii) the degree of inhibition of the DNA-dependent RNA polymerase are dependent on the presence of the amino sugar moiety of daunoseamine. The results are consistent with specific H bonding of the amino group of the sugar moiety with DNA as has been suggested earlier by Pigram et al. (Pigram, W. J., Fuller, W., and Hamilton, L. D. (1972), *Nature (London), New Biol. 235,* 17). Peptide derivatives substituted at the amino sugar function of daunorubicin lower the affinity of the drug to DNA and presumably interfere with the "full insertion" of the anthracycline drugs between base pairs of DNA. The significance of these findings in relation to the biological efficacy of daunorubicin and related derivatives as antileukemic agents is discussed.

The interaction specificities of daunorubicin (a potent antileukemic drug) and various anthracycline derivatives with nucleic acids have been the subject of numerous studies in recent years (Henry, 1974; DiMarco and Arcamone, 1975; Zunino et al., 1974; Dalgleisch et al., 1974; Kersten et al., 1966; Waring, 1970; Pigram et al., 1972). It is now generally recognized that the biological activity of these drugs involves inhibition of the cellular RNA- and DNA-dependent replication and transcription processes (Meriwether and Bachur, 1972; Hartmann et al., 1964; Ward et al., 1965; Mizuno et al., 1975). Unfortunately, the unfavorable cytotoxic properties of daunorubicin on cardiac tissues have limited its usefulness as an effective chemotherapeutic agent in the treatment of cancer in humans (Smith, 1969; Raskin et al., 1973; Halazun et al., 1974; Mhatre et al., 1971; Herman et al., 1970; Bachur et al., 1974; Chalcroft et al., 1973; Cornu et al., 1974). For this reason, considerable interest is being focused on the synthesis of potentially nontoxic derivatives.

The present work deals with comparative studies of the interaction specificities of salmon sperm DNA with daunorubicin (**1**) and two types of substituted derivatives, i.e., (i) at the amino sugar, **2–5**, and (ii) at the 9-keto methyl moieties, **6** and **7** (Chart I).

Experimental Section

The syntheses of the peptide derivatives **2–4** were carried out by the mixed anhydride procedure of Anderson et al.

† From the Department of Chemistry, University of Florida, Gainesville, Florida 32611 (E.J.G., D.G., R.E.F., R.R., R.L., S.W.P.) and the Department of Chemistry, Georgia State University, Atlanta, Georgia 30303 (W.D.W.). *Received October 8, 1975.* This work was supported by an institutional grant from the American Cancer Society and by Grants GM17503 and GM18653 from the U.S. Public Health Service and Grant GB16044 from the National Science Foundation.

‡ National Institutes of Health Career Development Fellow (1970–1975).

§ Undergraduate research participants, University of Florida.

Fellow of the Helen Hay Whitney Foundation (1973–1974); present address: Department of Medicine, Stanford Medical School, Palo Alto, Calif.

¶ Predoctoral Fellow, University of Florida, 1972–1976.

‡‡ On leave from the Department of Chemistry, Georgia State University (1974–1975).